

Bounds on large extra-dimensions from the LHC

arXiv:1101.4919

with

P.P. Giardino, G.F. Giudice, P. Lodone, A. Strumia

Roberto Franceschini

EPFL Lausanne

September 1st 2011

Outline

- Motivation
- Phenomenology
- Bounds on tree-level graviton exchange
- Real graviton emission
- Conclusions

Motivation and set-up

after all the hierarchy might be between two not so separated scales ...

This is what happens when gravity feels $D = 4 + \delta$ dimensions:

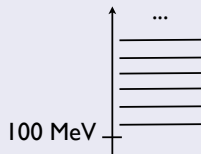
- $\bar{M}_{pl}^2 = \bar{M}_D^{2+\delta} \cdot V_{(\delta)}$ where $V \sim R^\delta$, $\bar{M} \equiv M/\sqrt{8\pi}$

$$R = 10^{12}, 10^{-3}, 10^{-12}, 10^{-15} \text{ m for } \delta = 1, 2, 4, 6$$

$$\frac{1}{R} = 10^{-21} \text{ eV}, 10^{-4} \text{ eV}, 20 \text{ KeV}, 7 \text{ MeV for } \delta = 1, 2, 4, 6$$

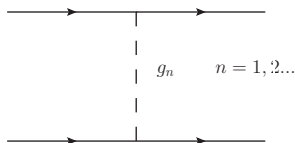
- KK expansions naively gives $m_{g_n} \sim \frac{n}{R}$
- astrophysics limits for gravitons below $O(100)$ MeV
(arXiv:hep-ph/0304029)
- can be avoided lifting the KK tower above $O(100)$ MeV with a modification of the metric of the ED (arXiv:hep-ph/0002001, hep-ph/0108115, hep-ph/0408320)

such modifications are irrelevant for a collider



Gravitons exchange

- KK states of the graviton tower can mediate $2 \rightarrow 2$ scattering



- Each graviton is weakly coupled, $\sim 1/M_{pl}$, but there are many KK (due to the large ED phase-space as $m_{KK} = p_{ED}$)
- The effect might be dominated by UV physics ($\delta > 2$)
- At the very least you can model the effect of tree-level exchange of gravitons with a dimension-8 operator

$$\mathcal{L} \supset c_T \mathcal{T} \equiv \frac{8}{M_T^4} \cdot \frac{1}{2} \left(T_{\mu\nu} T^{\mu\nu} + \frac{1}{\delta + 2} T^\mu{}_\mu T^\nu{}_\nu \right)$$

$pp \rightarrow \gamma\gamma, \ell\bar{\ell}, \dots$ and do not forget jj

Energy pays off to probe the dim-8: LHC7@2010 \gg TeVatron

$$\sigma = \left(\frac{2 \text{ TeV}}{M_T}\right)^8 \times \begin{cases} 12.5 \text{ pb} & \text{for } pp \rightarrow jj \quad \text{no search so far ...} \\ 10.4 \text{ fb} & \text{for } pp \rightarrow \mu^+\mu^- \quad \text{EXO-11-039} \\ 21.3 \text{ fb} & \text{for } pp \rightarrow \gamma\gamma \quad \text{EXO-11-038} \end{cases}$$

- $\ell\bar{\ell}$ and $\gamma\gamma$ roughly a cut-and-count in the high mass region
- jj has a larger rate, but cut-and-count is risky due to QCD uncertainties

$pp \rightarrow \gamma\gamma, \ell\bar{\ell}, \dots$ and do not forget jj

Energy pays off to probe the dim-8: LHC7@2010 \gg TeVatron

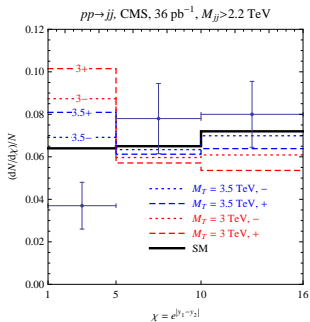
$$\sigma = \left(\frac{2 \text{ TeV}}{M_T}\right)^8 \times \begin{cases} 12.5 \text{ pb} & \text{for } pp \rightarrow jj \text{ no search so far ...} \\ 10.4 \text{ fb} & \text{for } pp \rightarrow \mu^+ \mu^- \text{ EXO-11-039} \\ 21.3 \text{ fb} & \text{for } pp \rightarrow \gamma\gamma \text{ EXO-11-038} \end{cases}$$

- $\ell\bar{\ell}$ and $\gamma\gamma$ roughly a cut-and-count in the high mass region
- jj has a larger rate, but cut-and-count is risky due to QCD uncertainties
- Bounds can be extracted from the angular distribution arXiv:0906.4819 (D0)
- $uu \rightarrow uu$ dominates at LHC $\Rightarrow jj$ is even better than at TeVatron

$\frac{d\sigma}{d\chi}$ angular distribution, $\chi \equiv \exp |y_1 - y_2|$

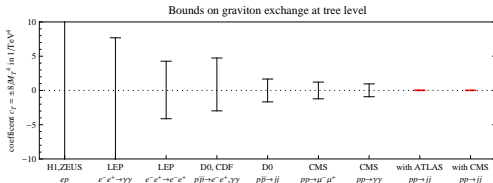
Being the mediator a spin-2 each vertex has a p_T^2 dependence as opposed to the p_T dependence of a spin-1.

- Signal gives more central events (small χ)



$M_T > 3.4 \text{ TeV}$ with $36/\text{pb}$, waiting for the update

- higher mass m_{jj} as \mathcal{L} increases
- smaller region in χ (if the detector allows)



arXiv:1103.3864,1102.2020

Virtual Gravitons in $\gamma\gamma$ and $\mu\bar{\mu}$ searches

$pp \rightarrow \mu\bar{\mu}$ with $\mathcal{L} \sim 1/\text{fb}$: $M_T > 2.3 \text{ TeV}$

Table 3: Observed 95% upper limits in TeV with respect to GRW and HLZ conventions for full model validity in \sqrt{s} and truncation at $M_{\text{gr}} = M_s$ (HLZ) or $M_{\text{gr}} = \Lambda_T$ (GRW).

	Λ_T [TeV] (GRW)	M_s [TeV] (HLZ)					
		$n=2$	$n=3$	$n=4$	$n=5$	$n=6$	$n=7$
ADD k-factor: 1.0							
Full	2.62	2.58	3.12	2.62	2.36	2.20	2.08
Truncated	2.56	2.58	3.10	2.56	2.27	2.09	1.95
ADD k-factor: 1.3							
Full	2.70	2.72	3.22	2.70	2.44	2.28	2.16
Truncated	2.66	2.72	3.20	2.66	2.37	2.17	2.02

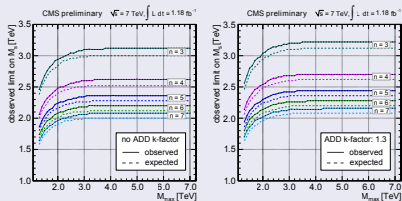


Figure 3: Observed 95% upper limits on M_s for different numbers of extra dimensions n with (Left) and without (Right) ADD k-factor.

EXO-11-039

$pp \rightarrow \gamma\gamma$ with $\mathcal{L} \sim 1/\text{fb}$: $M_T > 2.7 \text{ TeV}$

Table 2: Table of 95% CL lower limits on M_s (in TeV), as a function of the number of EDs in the HLZ convention for two different values of the ADD signal K factor. All limits are computed with a signal cross section truncated to zero when $\sqrt{s} > M_s$.

K factor	$n_{\text{ED}}=2$	$n_{\text{ED}}=3$	$n_{\text{ED}}=4$	$n_{\text{ED}}=5$	$n_{\text{ED}}=6$	$n_{\text{ED}}=7$
1.0	3.2	3.4	2.8	2.6	2.4	2.2
1.6	3.5	3.7	3.1	2.8	2.6	2.4

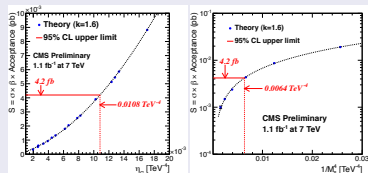


Figure 4: Signal cross section parameterization as a function of the strength of the ED effects, η_G (left) and as a function of $1/M_s^2$ for the $n_{\text{ED}} = 2$ case (right).

EXO-11-038

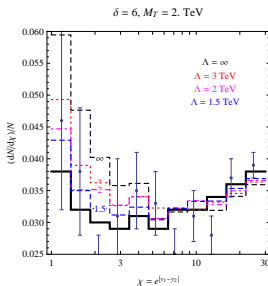
$\frac{d\sigma}{d\chi}$ angular distribution, $\chi \equiv \exp |y_1 - y_2|$

Being the mediator a spin-2 each vertex has a p_T^2 dependence as opposed to the p_T dependence of a spin-1.

- Signal gives more central events (small χ)

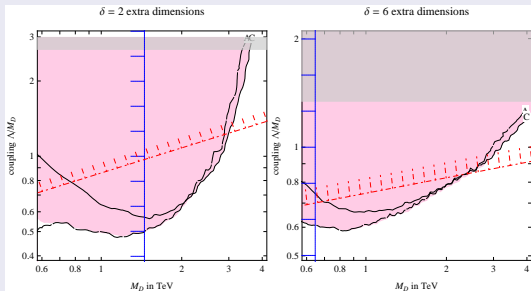
$$\mathcal{A} = \mathcal{S}_{\delta,\Lambda}(s) \left(T_{\mu\nu} T^{\mu\nu} - \frac{T^\mu{}_\mu T^\nu{}_\nu}{\delta + 2} \right)$$

$$\mathcal{S}_{\delta,\Lambda}(s) = \frac{1}{M_D^{\delta+2}} \int_{|q| < \Lambda} \frac{d^\delta q}{s - q^2 + i\epsilon}$$



$\frac{d\sigma}{d\chi}$ angular distribution, $\chi \equiv \exp |y_1 - y_2|$

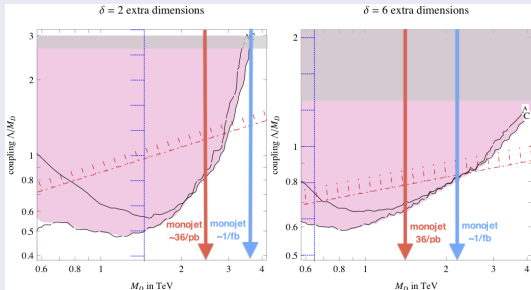
ATLAS and CMS with 36/pb



$\frac{d\sigma}{d\chi}$ angular distribution, $\chi \equiv \exp |y_1 - y_2|$

ATLAS and CMS with 36/pb plus monojet searches

EXO-11-058, EXO-11-059, ATLAS-CONF-2011-096, arXiv:1103.3864,1102.2020



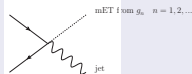
- ED pushed in the multi-TeV region

Extending the reach of ED searches

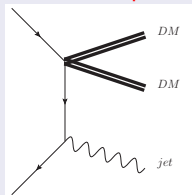
limits from $j+mET$ and $\gamma+mET$

- Extra-dimensions searches

EXO-11-058, EXO-11-059, ATLAS-CONF-2011-096



- dark matter production (see T. Tait)



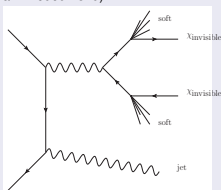
Sparse thoughts:

(personal set of open questions)

- **one or many** invisible body final states?
see R. Mahbubani and B. Gripaios on arXiv:1108.1800
- **continuous spectrum** of invisibles or just a single/multi body final state?

- any chance to catch difficult scenarios as **degenerate (N)LSP** in jet+mET+soft l s?

(Giudice, Han, Wang, Wang arXiv:1004.4901, Buckley, Randall, Shuve arXiv:0909.4549)



Conclusions

- No signal of large extra-dimensions so far (M_D constrained in the multi-TeV region)
- Best bounds on tree-level gravitons from the angular distribution in $pp \rightarrow jj$
- Monojet searches can be recycled for DM searches and more (discussion?)

$$S(s) = \frac{1}{M_D^{2+\delta}} \int_{|q|<\Lambda} \frac{d^4 q}{s - q^2 + i\epsilon} = \frac{\pi^{\delta/2} \Lambda^{\delta-2}}{\Gamma(\delta/2) M_D^{2+\delta}} F_\delta\left(\frac{s}{\Lambda^2}\right)$$

$$F_{\delta+2}(x) = x F_\delta(x) - \frac{2}{\delta}$$

$$F_1(x) = \frac{2}{\sqrt{x}} \operatorname{arctanh} \frac{1}{\sqrt{x}}, \quad F_2(x) = -\log\left(1 - \frac{1}{x}\right).$$

$$M_S(\text{Hewett})|_{\lambda=+1} = \sqrt{\frac{2}{\pi}} M_S(\text{HLZ})|_{n=4}$$

$$\Lambda_T = M_S(\text{HLZ})|_{n=4}.$$

Table 1. Lower limits at the 95% CL on the effective Planck scale, $M_S(\text{Hewett})$, in TeV, from searches for direct graviton production at LEP. Limits from $\sqrt{s} > 200$ GeV data are shown in normal font; limits from 189 GeV data are in *italics*; limits from 184 GeV data are in **bold** script.

Experiment	$e^+e^- \rightarrow \gamma G_{KK}$				$e^+e^- \rightarrow Z G_{KK}$					
	$n=2$	$n=3$	$n=4$	$n=5$	$n=2$	$n=3$	$n=4$	$n=5$	$n=6$	
ALEPH	1.10	0.86	0.70	0.60	0.52	0.35	0.22	0.17	0.14	0.12
DELPHI	1.25	0.97	0.79	0.68	0.59	N/A	N/A	N/A	N/A	N/A
L3	<i>1.02</i>	<i>0.81</i>	<i>0.67</i>	<i>0.58</i>	<i>0.51</i>	<i>0.60</i>	<i>0.38</i>	<i>0.29</i>	<i>0.24</i>	<i>0.21</i>
OPAL	<i>1.09</i>	<i>0.86</i>	<i>0.71</i>	<i>0.61</i>	<i>0.53</i>	N/A	N/A	N/A	N/A	N/A

Experiment	Process	+	-
LEP [7]	$e^+e^- \rightarrow \gamma\gamma$	0.93 TeV	1.01 TeV
LEP [8]	$e^+e^- \rightarrow e^+e^-$	1.18 TeV	1.17 TeV
H1 [9]	e^+p and e^-p	0.74 TeV	0.71 TeV
ZEUS [10]	e^+p and e^-p	0.72 TeV	0.73 TeV
CDF [11]	$p\bar{p} \rightarrow e^+e^-, \gamma\gamma$	0.99 TeV	0.96 TeV
DØ [11]	$p\bar{p} \rightarrow e^+e^-, \gamma\gamma$	1.28 TeV	1.14 TeV
DØ [12]	$p\bar{p} \rightarrow jj$	1.48 TeV	1.48 TeV
CMS at 7 TeV with 40/pb [13]	$pp \rightarrow \mu^-\mu^+$	1.6 TeV	1.6 TeV
CMS at 7 TeV with 36/pb [23]	$pp \rightarrow \gamma\gamma$	1.74 TeV	1.71 TeV
ATLAS at 7 TeV with 3.1/pb	$pp \rightarrow jj$	2.2 TeV	2.1 TeV
ATLAS at 7 TeV with 36/pb	$pp \rightarrow jj$	4.2 TeV	3.2 TeV
CMS at 7 TeV with 36/pb	$pp \rightarrow jj$	4.2 TeV	3.4 TeV

Experiment	Process	+	-
LEP combined [15]	$e^+e^- \rightarrow e^+e^-$	11.3	11.5
LEP combined [15]	$e^+e^- \rightarrow \mu^+\mu^-$	16.4	12.7
LEP combined [15]	$e^+e^- \rightarrow \ell^+\ell^-$	17.2	15.1
LEP combined [15]	$e^+e^- \rightarrow b\bar{b}$	15.3	11.5
H1 [9]	e^+p and e^-p	2.5	3.9
ZEUS [10]	e^+p and e^-p	4.6	5.3
DØ [16]	$p\bar{p} \rightarrow e^+e^-$	4.7	5.5
CDF [16]	$p\bar{p} \rightarrow \ell^+\ell^-$	4.5	5.6
CCFR [17]	νN scattering	3.7	5.9
DØ [16]	$p\bar{p} \rightarrow jj$	3.2	3.1
ATLAS at 7 TeV with 3.1/pb	$pp \rightarrow jj$	5.3	4.2
CMS at 7 TeV with 36/pb	$pp \rightarrow jj$	11	8.1
combined		22.4	15.7

Table 2. Loop-level graviton exchange: 96% CL limits on the coefficient $|c_T/4\pi|^{-1/2}$ (in TeV) of the dimension-6 operator T of eq. (3) for positive and negative values of c_T .